Dry sliding wear mechanisms of Ce in aluminum bronze coatings

Wensheng Li[a], Haimin Zhai[a*], Shuncai Wang[b], Shujie Liu[a], Robert Wood[b]

[a]*State Key Laboratory of Advanced Processing and Recycling of Nonferrous Metals, Lanzhou University of Technology, Lanzhou 730050, China*

[b]*National Centre for Advanced Tribology, Faculty of Engineering and the Environment, University of Southampton, Southampton, SO17 1BJ, United Kingdom*

Abstract:

A new type of cerium bronze coatings with aluminum as the main compound and over the solubility limit were successfully fabricated on a mild steel substrate by plasma spraying system. Scanning electron microscopy analysis showed that Ce refined the microstructure effectively, which resulted in an increase of average hardness. Ce stimulated the Fe element diffusion from the substrate to coating which resulted in the evolution of Fe-containing intermetallics from the FeAl (κ_2 phase) to Fe_3Al (κ_1 phase). This study also shows that a small amount of Ce (0.1 wt. %) added into the novel aluminum bronze coating can improve the abrasive wear-resistance by refining the microstructure and increasing the hardness of the coating, where the excess Ce (0.6 wt. %) addition will reduce the abrasive wear-resistance of the coating.

Keywords: Ce addition; Aluminum bronze coating; Microstructure; Hardness; Wear resistance

* Corresponding author:
E-mail address: hmzhai@lut.edu.cn (Haimin Zhai)

Introduction

Thermal spray is a technique that provides coatings for applications which require wear and corrosion protection. Recently, the aluminum bronze coatings deposited by electric arc spray, ion-plated and plasma spray have been developed as potential new candidates for manufacturing and repairing of metal forming dies [1-4]. In addition, Li et al. fabricated aluminum bronze coatings by using thermal sparying [5]. Recently, Xu et al. further developed a rare earth (RE) containing aluminum bronze coating of Cu-14Al-4.5Fe-Ni-RE for die material [6]. This novel bronze coating has a significantly higher the hardness (390-420 HV) and thus improved wear resistance, but its brittleness makes it difficult to be processed into the mould.

The previous studies have shown that a small amount of RE addition improves the wear-resistance and mechanical properties of high aluminum bronze coating [7-9]. Ce element, with strong chemical activities, can react easily with many impurity elements such as H, O, N, S, and Si, which has been used to clean up these impurities. Moreover, previous studies also demonstrated that small amount Ce addition can make the microstructure less porous, more compact and denser, leading to an increase of micro-hardness in the Ni/Co baized thermal spray coatings [10-15]. It also transforms the phase morphologies from needle-shape to small globular-shape [8]. However, few studies have looked at the effect of the Ce on the wear resistance of the aluminum bronze coating.

In this study, the high aluminum bronze coatings with different Ce contents (0 wt. %, 0.1 wt. % and 0.6 wt. % Ce, named as Ce-free, 0.1 wt. % Ce coating and 0.6 wt. % Ce coating) were prepared on the 1045 steel substrate by plasma spraying. The friction and wear behaviors of the high aluminum bronze coatings against stainless steel were investigated. The detailed investigations of the worn specimens and counterpart have been carried out with different Ce contents, in order to understand the tribological mechanism and the RE effects.

Experimental

Specimen preparation

Prior to the spraying of novel high aluminum bronze coatings, different Ce powders of the Ce-free and Ce (0.1 wt. %, 0.6 wt. %) were atomized (in the nitrogen atmosphere with cooling water) using our patented one-melted technique [15]. The chemical composition of Cu-14Al-4.5Fe-Ni alloy powders and 1045 steel substrate were listed in Table 1 and Table 2, respectively. The

average particle size of powders was about 110 ±15 μm. The alloy powders were then sprayed on the 1045 steel substrate by plasma spraying, and then cooled down in air. The size of the substrate is Φ200×30 mm. A detail of the plasma spraying process was shown in our recent work [16].

Table 1 Chemical composition of the Cu-14Al-4.5Fe-Ni alloy

Ingredients	Cu	Al	Fe	Co	Ni	Others
Weight percent (wt. %)	75~80	13~16	2.0~4.5	0.5-0.8	0.4~0.6	1.0~2.6

Table 2 Chemical composition of the substrate 1045 steel

Ingredients	Fe	Mn	C	Si	Ni	Cr	Cu	others
Weight percent (wt. %)	98.0~97.5	0.6~0.9	0.43~0.50	0.17~0.37	<0.25	<0.25	<0.25	<0.1

Microstructure characterization

The microstructures of the coatings were characterized by X-ray diffraction (XRD: Bruker D8), scanning electron microscopy (SEM: JSM6700F), and transmission electron microscopy (TEM, JEM3010, 300 kV). The SEM specimens were etched using a solution of 5 g $FeCl_3$, 10 ml HCl and 100 ml distilled water, and the TEM specimens were electro-polished with a solution of 20 % HNO_3, 15 % 2-butoxyethanol and 65 % methanol. The compositions of the coatings were analyzed by energy-dispersive spectroscope (EDS, OXFORD ISIS 300) and electronic probe microanalysis (EPMA, EPMA-1610). The topographical feature, micro-constitutes of the worn surface and the cross-sections of worn specimens were also analyzed by using the SEM, EPMA, and EDS, respectively.

Mechanical properties testing

The hardness of the coatings was tested by the Vickers HD1-187.5 Sclero-meter with a load of 4.9 N. To ensure accurate Vickers hardness measurement, the load is kept for 10s. In order to ensure the accuracy and repeatability of the testing results, three specimens were measured and averaged as a final result. A detail of the column-on-block wear testing procedure was shown in our recent work [13]. The size of the test column specimen and the counterpart (1Cr18Ni9Ti steel with a hardness of 200 HV) was 8 mm in diameter and 70 mm × 13.7 mm ×10 mm, respectively. Prior to friction testing, the contacting surfaces of the column specimens and block specimens were polished by using SiC to achieve an average surface roughness (Ra < 800 nm), and then the testing specimens were vacuum-dried and weighed. The wear tests were carried out with the

applied loads of 196 N, 294 N and 392 N at room temperature and without lubrication, respectively. Each wear testing lasted for 30 min with a sliding velocity of 0.2 ms^{-1} (corresponds to a sliding distance of 360 m). After friction testing, the weight loss was calculated by weight of the coating and counterpart samples with a balance accuracy of 0.1 mg.

Results

Microstructures

The microstructures of the novel aluminum bronze (Cu-14Al-4.5Fe-Ni-RE) coating with different Ce contents (0 wt. %, 0.1 wt. % and 0.6 wt. % Ce) were presented in Fig. 1. According to our previous work [17,18], the Ce-free coatings have four different phases: α phase (the light areas, fcc copper rich solid solution), β' phase (dark areas, the martensitic phase, Cu_3Al), κ_2 phases (various morphologies, intermetallic phase, FeAl), and the brittle γ_2-phases (intermetallic phase, located at grain boundaries), as shown in Fig. 1a. By adding 0.1 wt.% Ce, the coating structure transformed into a fine structure consisting of agglomerates of crystals with an approximately irregular net-shape/rod-like appearance, as shown in Fig. 1b. When the Ce content increased to 0.6 wt. %, the coating exhibited dendrite shape aligned with much bigger intermetallics than that of the 0.1 wt. % Ce coating, as shown in Fig. 1c. All results indicated that Ce additions can adjusted the relative content, size, shape and distribution of the phases in microstructure of the coatings. The EDS analysis of the coating with different Ce contents is presented in Table 3. The results showed that the Fe element in coating gradually increased with the addition of Ce.

The XRD results of the coatings with different Ce contents were presented in Fig. 2. Compared with the Ce-free coating, the 0.1 wt. % Ce coating had broader peaks, indicating that the grain size of the coating microstructure was effectively reduced with Ce. In addition, several other Fe_3Al (κ_1), Fe_3Mn_7 phase peaks gradually pronounced, particularly κ_1 phase associated with the peak at 45.6°. With the increase of the Ce content, more peaks corresponding to κ_1 phase appeared which indicated the increase of the κ_1 phase.

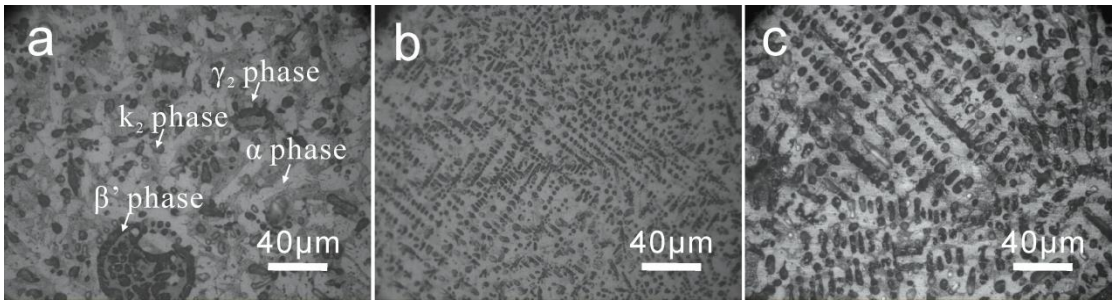

Fig. 1. Microstructure photographs of the aluminum bronze coatings: (a) Ce-free, (b) 0.1 wt. % Ce, (c) 0.6 wt. % Ce.

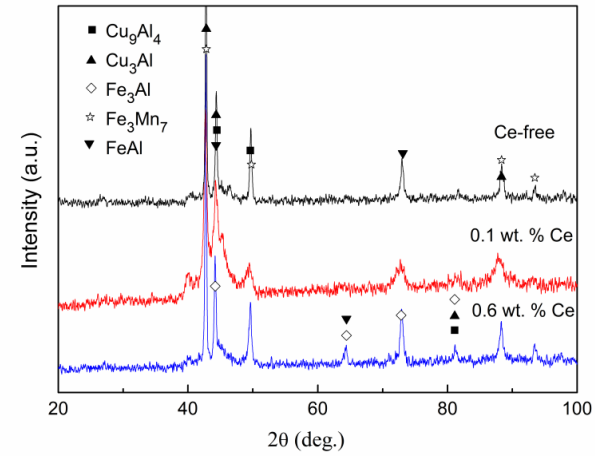

Fig. 2. XRD patterns of the aluminum bronze coatings with different Ce contents (Ce-free, 0.1 wt. % and 0.6 wt. % Ce).

Table 3 Chemical compositions of the aluminum bronze coatings with different Ce contents (Ce-free, 0.1 wt. % and 0.6 wt. % Ce).

Coating	Chemical analysis, wt. %				
	Cu	Al	Fe	Ce	Others
0 wt. % Ce	67.5	9.9	20.0	0	2.6
0.1 wt. % Ce	66.7	10.1	20.5	0.1	2.5
0.6 wt. % Ce	60.6	10.1	26.7	0.6	1.9

Hardness

The hardness of the coatings with different Ce contents was presented in Fig. 3. The average hardness of the Ce-free, 0.1 wt. % Ce and 0.6 wt. % Ce coatings were 281.5±8.0 HV, 304±9.5 HV, and 326±7.5 HV, respectively. Compared with the Ce-free coating, the average hardness of the 0.1 wt. % Ce and 0.6 wt. % Ce coating increased about 7.99 % and 15.8 %, individually. It showed that Ce addition can enhance the hardness of the novel aluminum bronze coatings.

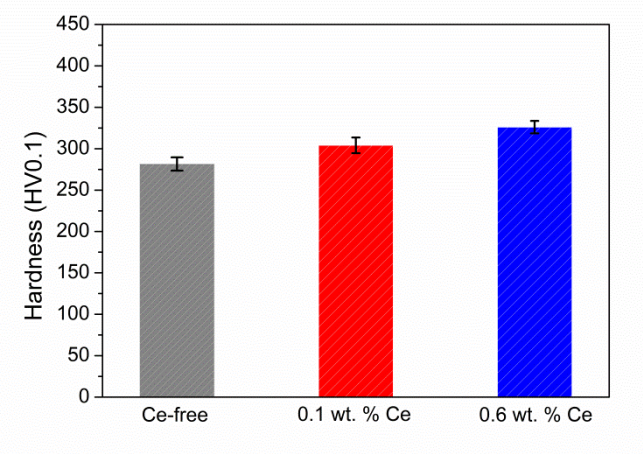

Fig. 3. Hardness of the aluminum bronze coatings with different Ce contents (Ce-free, 0.1 wt. % Ce and 0.6 wt. % Ce).

Tribological properties

Fig. 4a shows the dynamic coefficient of friction (COF) of the coatings with different Ce contents at loads of 196 N, 294 N and 392 N, respectively. Compared with the coating contained Ce (0.1 wt. % or 0.6 wt. %), the Ce-free coating had the lowest COF at 196 N but higher COF at loads of 294 N and 392 N. The 0.1 wt. % Ce coating generated firstly constant and with lower COF value at loads of 294 N and 392 N, indicating that the effect of the applied load on the COF on the 0.1 wt. % Ce coating was inconspicuous. The COF of the coating increased when Ce content increases to 0.6 wt. %, suggesting that the COF can only be effectively reduced by small adequate amounts of Ce.

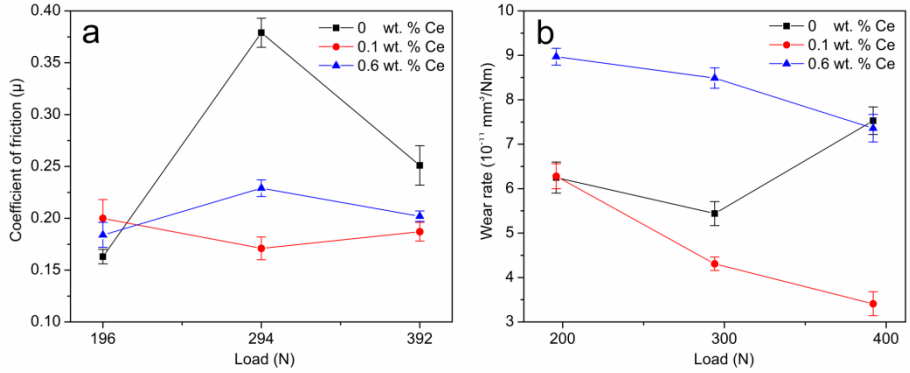

Fig. 4. Aluminum bronze coatings with different Ce: (a) COF under different loading, (b) wear rate under different loading.

Fig. 4b showed the wear rate of the coatings with different Ce contents at loads of 196 N, 294 N and 392 N, respectively. Similar to the evolution of COF, the Ce-free coating also had a low wear rate at the load of 196 N and high wear rate at the load of 392 N. For the 0.1 wt. % Ce

coating, the wear rate continues to decrease with the increase of load, indicated that the wear resistance can be improved by a small amount of Ce. However, when the Ce content increased to 0.6 wt. %, the coating had higher wear rate at the loads particularly of the 196 N and 294 N, which suggested that over amount Ce would lead to a poor wear-resisting performance.

Characterization of the worn surface

To reveal the effects of Ce addition on the friction and wear mechanism of the novel aluminum bronze coatings, the specimens were investigated by SEM. The morphologies of worn surfaces of the coating specimens (Ce-free, 0.1 wt. % Ce, and 0.6 wt. % Ce) are shown in Figs. 5-7, respectively.

Fig. 5 showed the worn surfaces morphologies of the Ce-free coating under different loads. Under the applied load of 196 N, the parallel scratches with very shallow grooves distributed on the surfaces (Fig. 5a), which indicated that the abrasive wear was the main mechanism. When the load increased to 294 N, irregular pits and large particles appeared on the surfaces. This suggested that significant adhesion and deformation wear occurred, which was evidenced by large debris being detached from the coating, as shown in the inset of Fig. 5b. All those results demonstrated that the wear mechanism was a combination of adhesion and abrasive grain abrasion. When the load increased to 392 N, large grey debris and irregular grooves distributed on the worn surface (Fig. 5c), which represented the splat delamination as the main wear mechanism.

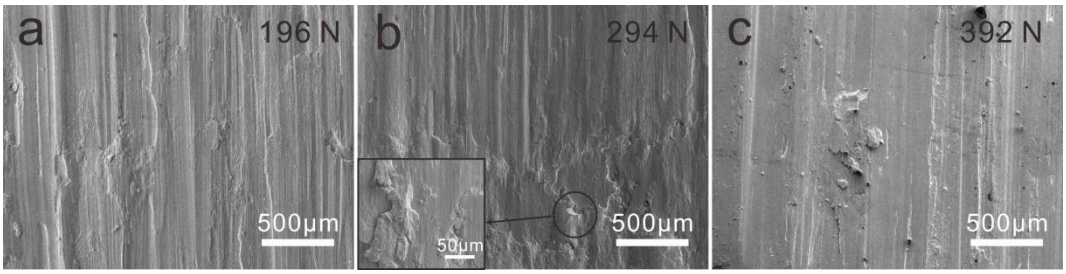

Fig. 5. Wear surfaces of Ce-free aluminum bronze coating under different applied load: (a) 196 N; (b) 294 N; (c) 392 N.

Fig. 6 showed the worn surface morphologies of 0.1 wt. % Ce coating under different loads. It can be seen that the surface was much smoother with a few debris attached within the grooves. This suggests that the main abrasion mechanism was mild abrasive wear, and almost independent with the increase of loads (see Figs. 6b and 6c). With the load increased, some additional wear mechanisms were involved. Very little debris was distributed on the worn surface of the coating under load of 196 N, and mild fatigue bulge appeared on the worn surface of the coating under

load of 294 N. When the load increased to 392 N, it showed the plastic deformation by sliding and flaky debris by fatigue [17], as shown in Fig 6c, which indicated that mild fatigue abrasion occurred on the worn surface.

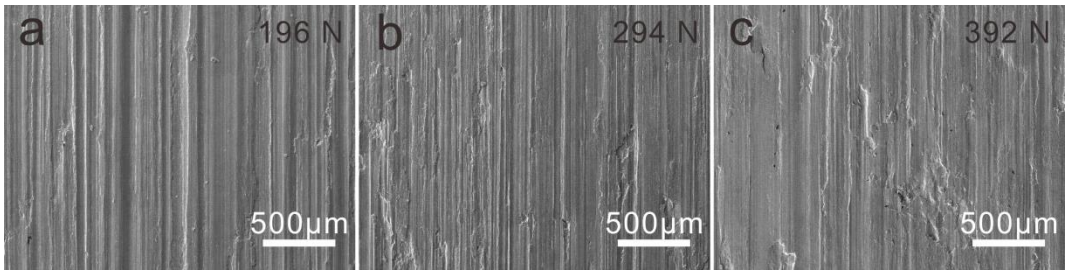

Fig. 6. Wear surfaces of 0.1 wt. % Ce aluminum bronze coating under different applied load: (a) 196 N; (b) 294 N; (c) 392 N.

Fig. 7 showed the worn surface morphologies of 0.6 wt. % Ce coating under the loads of 196 N, 294 N and 392 N, respectively. Compared with the 0.1 wt. % Ce coating, the grooves on the worn surface of 0.6 wt. % Ce coating became non-uniform and much deeper. Even under relative lower load of 196 N, wide grooves like wedge shapes with pointy tips and wide base caused by hard particles also distributed on the worn surface (inset of the Fig. 7a), suggested that the adhesion wear was the main wear mechanism. When load increased to 294 N, lots of debris like the roller kneaded covered on the worn surface. By contrast, the worn surface of the 0.1 wt. % Ce coating only had few of debris, as shown in Fig. 6b. The EDS results revealed that the debris was composed of copper and alumina oxides, suggested that the cohesion of the debris was repeatedly softened and melted by frictional heating [19]. When load increased to 392 N, it was found that the deposited debris had an obvious effect on the morphology of worn surface. However, in the Ce-free coating and 0.1 wt. % Ce coating, the effect of debris was not obvious under the same load conditions, as shown in Figs. 5c and 6c.

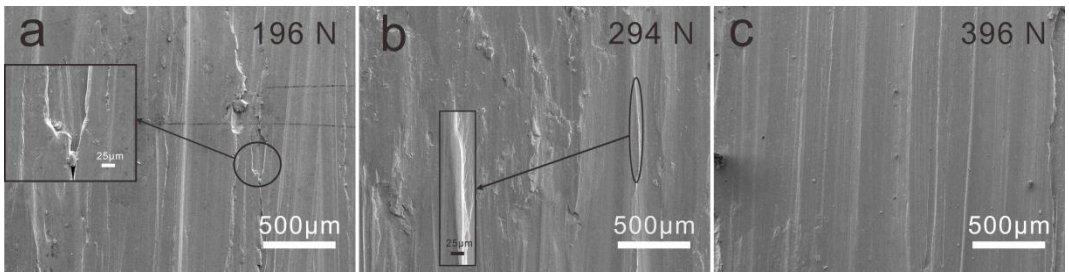

Fig. 7. Wear surfaces of 0.6 wt. % Ce aluminum bronze coating under different applied load: (a) 196 N; (b) 294 N; (c) 392 N.

Characterization of the worn cross-section surface

Cross-section examination of the worn surface can revealed the presence of different layers in the subsurface of the coatings. Fig. 8 showed that SEM images of the coatings after friction testing upon 294 N. For all the coatings, it can be seen that a heavily deformed layer (henceforth referred to as “HDL”) appeared beneath the surface, which was identified by numerous slip traces on an etched surface [20]. For the Ce-free, 0.1 wt. % Ce, and 0.6 wt. % Ce coatings, the thickness of the HDL was about 73.31 μm, 44.26 μm and 179.11 μm, respectively. Besides, for the Ce-free and 0.6 wt. % Ce coatings, it can be found that the HDL was capped by a thinner layer, where the slip traces and characters were no longer visible, which was named mechanically mixed layer (henceforth referred to as “MML”) [21]. Hence, the subsurfaces of the Ce-free and 0.6 wt. % Ce coatings consisted of MML, HDL and undeformed layer, as shown in Fig. 8a and c. However, for the 0.1 wt. % Ce coating, such a sequence was barely observed in the subsurface, indicated that the friction and wear mechanism of the 0.1 wt. % Ce coating was significantly different from that of Ce-free and 0.6 wt. % Ce coatings.

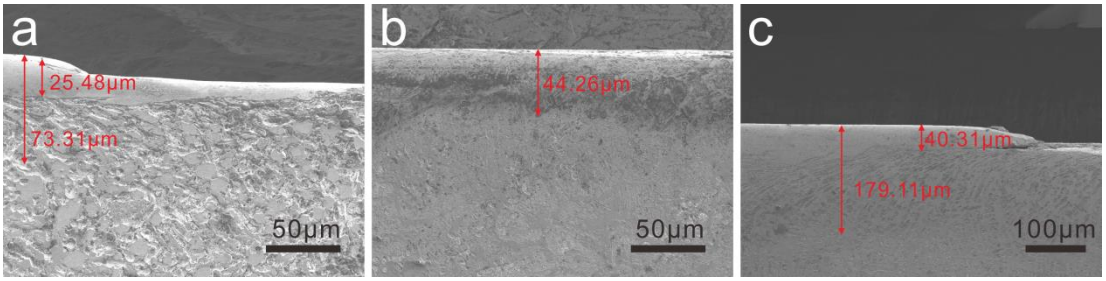

Fig. 8. Longitudinal section of the coatings after wears testing upon 294 N: (a) Ce-free; (b) with 0.1 wt. % Ce; (c) with 0.6 wt. % Ce.

Discussion

In engineering applications where metal materials are in contact with each other, friction and wear are two of the most important tribological issues to be considered, and the low COF and wear rate are no doubt desirable targets. As shown in Fig. 4a, the COFs of all coatings upon 196 N load were approximately equivalent at a very low values of 0.15~0.2, suggesting that the effect of the coating microstructure on the COF was not critical under low loading conditions. When the load increased to 294 N, the COF of the Ce-free coating and the 0.6 wt. % Ce coating increased rapidly, especially the COF of the Ce-free coating almost doubled. However, the COF of the 0.1 wt. % Ce coating reduced sharply, indicating that the microstructure of the coatings significantly affected the frictional behavior at 294 N loads. This phenomenon is mainly attributed to the modification of coating microstructure due to Ce addition. The present results indicate that the 0.1 wt. % Ce

coating exhibited the lower COF and wear rate than that of the Ce-free coating and 0.6 wt. % Ce coating (as shown in Fig. 4), which is particularly appealing as it is directly pertinent to engineering applications. However, friction and wear behavior of this novel high aluminum bronze coating appears to be slightly complicated as the increase of the Ce content and loading. The possible origins of the apparently low value of the COF and wear rate will be discussed further.

Fig. 1 shows that the microstructure of the novel aluminum bronze Cu-14Al-4.5Fe-Ni coating was strongly influenced by adding different Ce contents. As the Ce content increased from 0 wt. % to 0.6 wt. %, the microstructure morphologies of coating transferred from dendrite-shape or needle-like grains with high aspect ratio to a fine structure consisting of agglomerate crystals. Generally, the refining and purifying effect of the rare earth elements can make the alloys/coatings denser and grains finer [16]. According to our previous studies, the grain refinement is mainly attributed to the formation of the CeO_2 [16]. Since the melting point of CeO_2 (2500℃) is much higher than that of Cu-14Al-4.5Fe-Ni powder (1085℃), the CeO_2 cannot be melted during the spraying process, and thus may act as heterogeneous nucleation sites for crystallization. Besides, the high-melting CeO_2 particles were also pushed to the grain boundaries by the solid/liquid interface during solidification, as observed in other metal matrix composites [21]. Then the segregated CeO_2 particles at the grain boundaries tended to hinder the further grain growth by pinning the grain boundaries. Moreover, the EDS results confirmed that Ce stimulated the Fe element transfer from the substrate to the coating, resulted in the preferential formation of κ_1 phase, which also provided heterogeneous nucleation sites for crystal nucleation. When the Ce content in the coating increased to 0.6 wt. %, more Fe element was transferred from substrate into coating, thereby inducing more κ_1 phase formed and grown inside the coating, as shown in Figs. 2 and 9. It was also noted that when the Ce element content exceeded its solid solution limit [16, 18], the Ce_2Fe_{17} phase will form during the spraying process (Fig. 2). The newly formed Ce_2Fe_{17} phase also can effectively increase the nucleation rate of the κ_1 phase, and then further leaded to the refinement of the grain of the coating (Fig. 1c). On the other hand, the formation of the Fe-containing intermetallic phase also contributed to the increase of the coating hardness. As mentioned in section 3.1, the selected area electron diffraction (SAED) images (the Fig. 9a and b), show the κ_1 phase was almost absent in the Ce-free coating and only κ_2 phase was detected by XRD (Fig. 2) and TEM (Fig. 9). With the Ce addition, more κ_1 phase appeared in the 0.1 wt. % Ce

coating and 0.6 wt. % Ce coating (Fig. 9b). Since the κ_1 phase had a higher hardness (> 700 HV) than that of the κ_2 phase (> 650 HV), therefore, as the Ce content in the coating increased, the hardness of the coating slightly increased [18]. From Fig. 1, it can be seen that all coatings contain κ phases which are surrounded by soft β' phase (290-407 HV) and γ_2 phase (360-570 HV). The hard κ phase on the grinding surface bear the normal load and soft phases played a support role.

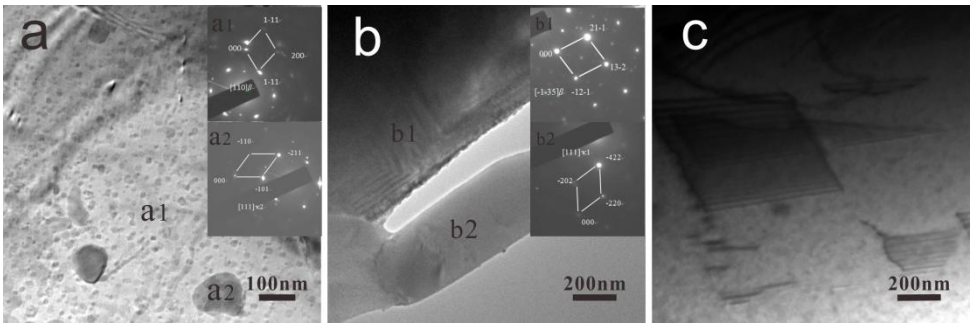

Fig. 9. The TEM images of the coatings: (a) Ce-free coating (inset are the corresponding SAED patterns of the Position a1and a2); (b) 0.6 wt. % Ce coating (inset are the corresponding SAED patterns of the Position b1and b2); (c) 0.6 wt. % Ce coating with stacking faults.

As mentioned previously, Ce additions can significantly refine the coating grain structure, resulting in an increase in coating hardness, as shown in Figs. 1 and 3. According to the Archard wear law for dry wear [15], the wear rate of the material is inversely proportional to its hardness. Therefore, compared with Ce-free coating, it can be found that the 0.1 wt. % Ce coating had lower wear rate under the loads of 294 N and 392 N. However, the 0.6 wt. % Ce coating had an unexpectedly poor wear resistance although it had the highest hardness. The reasons for this phenomenon will be discussed in detail below.

For the Ce-free coating, the morphology and size of eutectics (β', γ_2) and intermetallic (κ_2 phase) were not the same and their distribution was not uniform (Fig. 1). In particular, the hard κ_2 intermetallic phase with more complex structure was blocked in knots with a globular-shape (Fig. 9a). Upon sliding, the high load made the κ_2 phase bonding with counterpart steel, which leads to the wear rate of Ce-free coating increased significantly with the load increase, as shown in Fig. 4b. The increased wear rate of Ce-free coating under high loads should be attributed to the composition segregation in solidification grain boundary of coating which reduced the resistance of crack propagation [16], and then the soften matrix was easily stretched and scraped by the debris. The EDS analysis showed that Fe element changed to 33.25 wt. % in the worn surface of the Ce-free coating, which confirmed that the adhesive wear of the Ce-free coating occurred at

294 N. As shown in Fig. 5, with the load increased, the morphologies of Ce-free coating indicated the change from adhesive wear to splat delamination.

For the 0.1 wt. % Ce coating, the addition of Ce not only increased the hardness of the coating, but also increased the hardness of the coating by promoting the precipitation of the hard κ_1 phase, as shown in Figs. 1-2. Compared with Ce-free coating, wear rate of the 0.1 wt. % Ce coating had a lower value under 294 N and 392 N, and remained constant with the applied load increased from 196 N to 392 N. This was mainly due to trace Ce element addition which can strengthened the grain boundary and increased deformation resistance of the coating by making the coating structure denser and uniform. Hence, as shown in the Fig. 8, compared with Ce-free coating, the thickness of the HDL significantly reduced about 31 %, and no MML was found in the subsurface of the 0.1 wt. % Ce coating. Besides, the precipitated hard κ_1 phase on the grinding surface can bear the normal load and reduced the adhesion between coating and counterpart steel. As a consequence, compared with Ce-free and 0.6 wt. % Ce coatings, the 0.1 wt. % Ce coating had a lowest wear rate under 294 N and 392 N. Moreover, the homogeneous structure made crack propagation harder, hence there was no cracks appeared on the cross-section of the coating, as shown in Fig. 8b.

For the 0.6 wt. % Ce coating, the excess Ce addition made the size and the quantities of κ_1 phase increased obviously (Fig. 1c, Fig. 2 and Fig. 9b), which led to the boundary of the κ_1 phase being more brittle. When the transient temperature caused by friction was high enough to soften the surface, the hard κ_1 phase particle would easily detach from the matrix to be the debris. Then hard debris would plough the surface of coating and result in a deep groove on the worn surface, as shown in Fig. 7c. Moreover, the excess Ce addition also leads to slightly increased and the depth ploughed by the bigger hard debris also increased. Hence, the morphology of worn surface was dependent on the size of the hard debris [22]. The worn surface of the 0.6 wt. % Ce coating as shown in Fig. 7c, compared with Ce-free (Fig. 5) and 0.1 wt. % Ce (Fig. 6) coatings, had been cut and ploughed by the hard debris of κ_1 phase and thus its worn surface become smoother. Besides, larger κ_1 particles in the HDL region and the layered $\alpha+\kappa_1$ structure formed in material were the preferential sites for the cracks' nucleation. As shown in Figs. 8c and Fig. 10, cracks are observed between the HDL and the MML. Research by Shi et al. [23] proved that some cracks or pores can appear around larger κ particles in the deformed region of the as-received material. According to our previous studies [14], the addition of Ce could reduce the stacking fault energy (SFE) of the

Cu-Al alloy as shown in Fig. 9c. Hirth [24] also found that the low SFE softened the materials by dynamic work. Therefore, 0.6 wt. % Ce coating with low SFE could be more prone to plastic deformation. With continued dry sliding, the transferred particles deformed severely and mixed with the mutilated lamellar of the bronze. Since the 0.6 wt. % Ce coating contained more hard particles to transferred on the counter-face, the MML in the subsurface of the 0.6 wt. % Ce coating was thicker than that of the Ce-free and 0.6 wt. % Ce coatings (Fig. 8), which corresponded to a higher wear rate. Therefore, the COF and wear rate of the 0.6 wt. % Ce coating was greater than that of the 0.1 wt. % Ce coating.

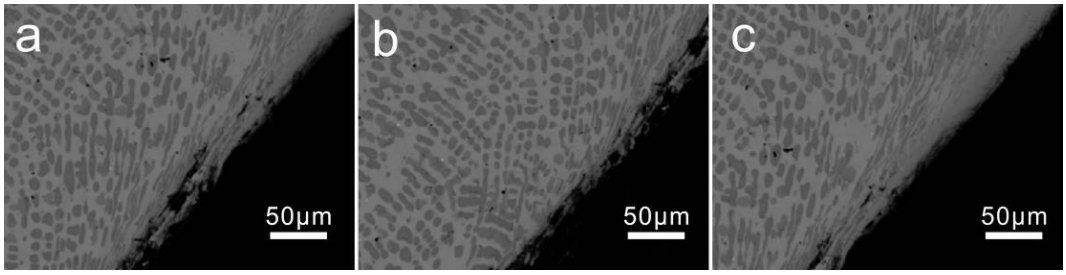

Fig. 10. The cracks on the cross-section surface of the 0.6 wt. % Ce coating which between the HDL and MML after wears testing upon 294 N.

On the other hand, the oxides produced during the friction process also have a significant influence on the COF of the coatings. In the sliding process, the transient temperature due to the friction was high enough to produce the oxidation on the surface of the wear track [25]. Under the lower normal load and the shear force, the oxides can be easily broken and moved out from the worn surface. In the course of the cyclic repetition of oxide generated, fracture and removed, some oxides were deposited on the wear track, which can effectively reduce the wear of the coating. With the load increased, the oxides are broken and transferred onto the coating surface. As shown in Fig. 11, the surfaces of the counterpart steel were covered by a layer of the coating materials, which means that materials had been transferred from the surface of the coating to the counterpart steel. The EDS analysis of the counterpart surface also confirmed the transfer of elements from the coating to the counterpart surface. It should be noted that there was few transferred particles on the counter steel surfaces the 0.1 wt. % Ce coating. As shown in Fig. 10b, the counter steel surfaces the with 0.1 wt. % Ce coating was much smoother than that of the Ce-free and 0.6 wt. % Ce coatings. However, when increased to 0.6 wt. % Ce, the transferred metal on the counterpart steel surface retransferred back to the surface of coating, as shown in Fig. 10c. This observation was also can be proved by the XRD analysis of the components of the coating's surface after

testing. From Figs. 2 and 11, the main components of the surface of the Ce-free, 0.1 wt. % Ce and 0.6 wt. % Ce coatings after testing were similar, except for the $AlCrFe_2$ and $Al_{43}Cr_7$ phase were found in the 0.6 wt. % Ce coating. Since the Cr element only existed in the counterpart steel, it clearly confirmed that the transferred metal on the counterpart steel surface retransferred back to the surface of coating. All these results leaded that the conversion of a sliding situation transferred from a two-body wear situation to a three-body (abrasive) wear situation, therefore, the wear rate of 0.6 wt. % Ce coating was greatly increased caused by the adhesion and abrasion of hard particles.

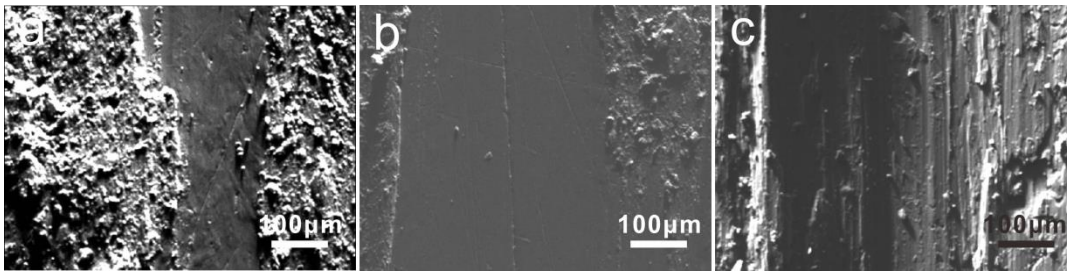

Fig. 11. Counter steel surface sliding with coatings under 294N: (a) Ce-free; (b) with 0.1 wt. % Ce; (c) with 0.6 wt. % Ce.

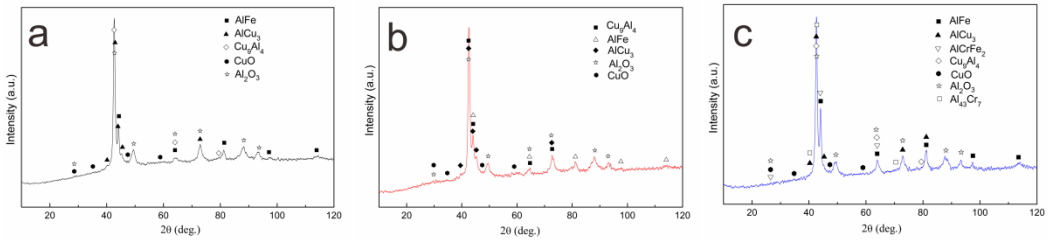

Fig. 12. XRD image of novel aluminum bronze with different Ce contents: (a) Ce-free; (b) with 0.1 wt. % Ce; (c) with 0.6 wt. % Ce.

Conclusions

The dry sliding tribological behaviors and wear mechanisms of aluminum bronze coatings with different Ce content (Ce-free, 0.1 wt. % and 0.6 wt. %) have been studied in detail under different loads (196 N, 294 N and 392 N). The main conclusions are as follows:

(1) The coatings with and without Ce both have the same types of phases - $\alpha+\beta'+\gamma_2$ phase and κ (Fe_3Al, FeAl and Fe_3Mn_7) phase. A trace of Ce (0.1 wt. %) addition refined the microstructure and uniform the composition. In contrast, the excess Ce addition (~ 0.6 wt. %) led to high κ_1 phase precipitation followed by growth to a large size. The increase of the coating hardness is because of the microstructure refinement. The interface adhesion is beneficial from Fe diffusion from the 1045 carbon steel substrate.

(2) A wide range of normal loads, from 196 N to 392 N, were employed to assess the friction and anti-wear properties. The results showed that the aluminum bronze coating with a small amount of Ce (0.1 wt. %) addition exhibited considerable potential as a high wear-resistance performance coating for the drawing and rolling dies. However, the 0.6 wt. % Ce addition coating exhibited an unsatisfied tribological performance, because too much κ_1 phase in 0.6 wt. % Ce coating intensified the tendency of the abrasion wear.

(3) Both 0.1 and 0.6 wt. % Ce coating has low coefficient of friction of 0.15-0.2. However, Ce has different effects on wear resistance. The 0.6 wt. % Ce coating had a poor wear rate though the 0.1 wt. % Ce coating showed a much improved wear resistance.

(4) Under dry sliding condition, a trace of Ce strengthened the grain boundary, increased the resistance of deforming, and prevented the crack propagation, which suggested that coating with 0.1 wt. % Ce could be applied in industry.

Acknowledgements

This investigation was supported by the supporting program of National Natural Science Foundation of China (51674130) and International science and technology cooperation program of China (2015DFR51090, 2016YFE0111400), the national high-end foreign experts program of China (GDT20186200331), the supporting program of Gansu province (1604WKCA008, 17YF1WA159), the International science and technology correspondent program of Gansu province (17JR7WA017).

References

[1] Guo X, Zhang G, Li W, Gao Y, Liao H, Coddet C (2009) Investigation of the microstructure and tribological behavior of cold-sprayed tin-bronze-based composite coatings. Appl. Surf. Sci. 255:3822-3828.

[2] Amokrane BM, Abdelhamid S, Youcef M, Abderrahim B, Nedjemeddine B, Ahmed M (2011) Microstructural and Mechanical Properties of Ni-Base Thermal Spray Coatings Deposited by Flame Spraying. Metall. Mater. Trans. B. 42:932-938.

[3] Ghorbani M, Mazaheri M, Afshar A (2005) Wear and friction characteristics of electrodeposited graphite-bronze composite coatings. Surf. Coat. Tech. 190:32-38.

[4] Sundquist HA, Matthews A, Teer DG (1980) Ion-plated aluminum bronze coatings for sheet metal forming dies. Thin solid films 73:309-314.

[5] Li WS, Liu Y (2012) Effect of Ce on wear behavior of plasma spray welded novel aluminum bronze coatings. Adv. Mater. Res. 418:831-834.

[6] Xu JL, Wang ZP, Chen C, La PQ (2004) Research into a new high-strength aluminum bronze alloy. Int. J. Mater. Prod. Tec. 21:443-453.

[7] Wang Y, Kovacevic R, Liu J (1998) Mechanism of surface modification of CeO in laser remelted alloy spray coating. wear 221:47-53.

[8] Cheng YL, Zheng CQ, Zhang Z, Cao FH, Li JF, Zhang JQ, & Wang JM (2002) The preparation and properties of iron base self-fluxing alloy spray-welding coatings with different rare earths and chromium content. J. Mater. Sci. 37:4589-4595.

[9] Wang KL, Zhang QB, Sun ML, Wei XG, Zhu YM (2001) Rare earth element modification of laser-clad nickel-based alloy coatings. Appl. Surf. Sci. 174:191-200.

[10] Han BL, Lu XC (2009) Effect of La_2O_3 on microstructure, mechanical and tribological properties of Ni-W coatings. Chinese. Sci. Bull. 54:4566-4570.

[11] Yi W, Zheng CQ, Fan P, Cheng SH, Li W, Ying GF (2000) Effect of the rare earth on oxidation resistance of iron base fluxing alloy spray-welding coating. Journal of Alloys and Compound, 311(1):65.

[12] Wang KL, Zhu YM, Zhang QB, Sun ML (1997) Effect of rare earth cerium on the microstructure and corrosion resistance of laser cladding nickel base alloy coatings. Journal of Materials Processing Technology, 63(1-3):563.

[13] Zhang ZY, Wang ZP, Liang BN (2005) Effect of CeO_2 on the microstructure and bond strength of Fe-Ni-Cu alloy. Journal of Rare Earths, 23(1):73.

[14] Zhao T, Cai X, Wang SX, Zheng SA (2000) Effect of CeO_2 on the microstructure and corrosive wear behavior of laser-cladded Ni/WC coating. Thin Solid Films, 379(1-2):128.

[15] Li WS, Wang ZP, Lu Y, Yong G, Xu J (2006) Preparation, mechanical properties and wear behaviors of novel aluminum bronze for dies. T. Nonferr. Metal. Soc. 16: 607-612.

[16] Li WS, Lu Y, Yuan KX, Yuan CG (2011) Effects of cerium on microstructure and bonding strength of Cu-14Al-4.5Fe bronze plasma sprayed coating. J. Rare. Earth. 29:363-369.

[17] Li WS, Wang ZP, Lu Y, Jin YH, Yuan LH, Wang F (2006) Mechanical and tribological properties of a novel aluminum bronze material for drawing dies. Wear 261:155-163.

[18] Li WS, Wang SC, Ma C, Wang ZP (2012) An electron microscopy study of the effect of Ce on plasma sprayed bronze coatings. Journal of Physics: Conference Series 371:012085

[19] Li Y, Ngai TL, Xia W (1996) Mechanical, friction and wear behaviors of a novel high-strength wear-resisting aluminum bronze. Wear 197:130-136.

[20] Singh JB, Cai W, Bellon P (2007) Dry sliding of Cu-15wt%Ni-8wt%Sn bronze: Wear behavior and microstructures. Wear 263:830-841.

[21] Zhao T, Cai X, Wang SX, Zheng SA (2000) Effect of CeO_2 on microstructure and corrosive wear behavior of laser-cladded Ni/WC coating. Thin Solid Films 379:128-132.

[22] Mølgaard J (1976) A discussion of oxidation, oxide thickness and oxide transfer in wear. Wear 40:277-291.

[23] Shi Z, Bloyce A, Sun Y, Bell T (1996) Influence of surface melting on dry rolling-sliding wear of aluminum bronze against steel. wear 198:300-306.

[24] Hirth JP, Rigney DA (1976) Crystal plasticity and the delamination theory of wear. wear 39:133-141.

[25] Kalin M (2004) Influence of flash temperatures on the tribological behavior in low-speed sliding: a review. Mat. Sci. Eng. A. 374:390-397.

high-strength wear-resisting aluminum bronze. Wear 197:130-136.

[16] Singh JB, Cai W, Bellon P (2007) Dry sliding of Cu-15wt%Ni-8wt%Sn bronze: Wear behavior and microstructures. Wear 263:830-841.

[17] Zhao T, Cai X, Wang SX, Zheng SA (2000) Effect of CeO_2 on microstructure and corrosive wear behavior of laser-cladded Ni/WC coating. Thin Solid Films 379:128-132.

[18] Mølgaard J (1976) A discussion of oxidation, oxide thickness and oxide transfer in wear. Wear 40:277-291.

[19] Shi Z, Bloyce A, Sun Y, Bell T (1996) Influence of surface melting on dry rolling-sliding wear of aluminum bronze against steel. wear 198:300-306.

[20] Hirth JP, Rigney DA (1976) Crystal plasticity and the delamination theory of wear. wear 39:133-141.

[21] Kalin M (2004) Influence of flash temperatures on the tribological behavior in low-speed sliding: a review. Mat. Sci. Eng. A. 374:390-397.

Figure 2

Click here to download Figure Fig. 2.tif

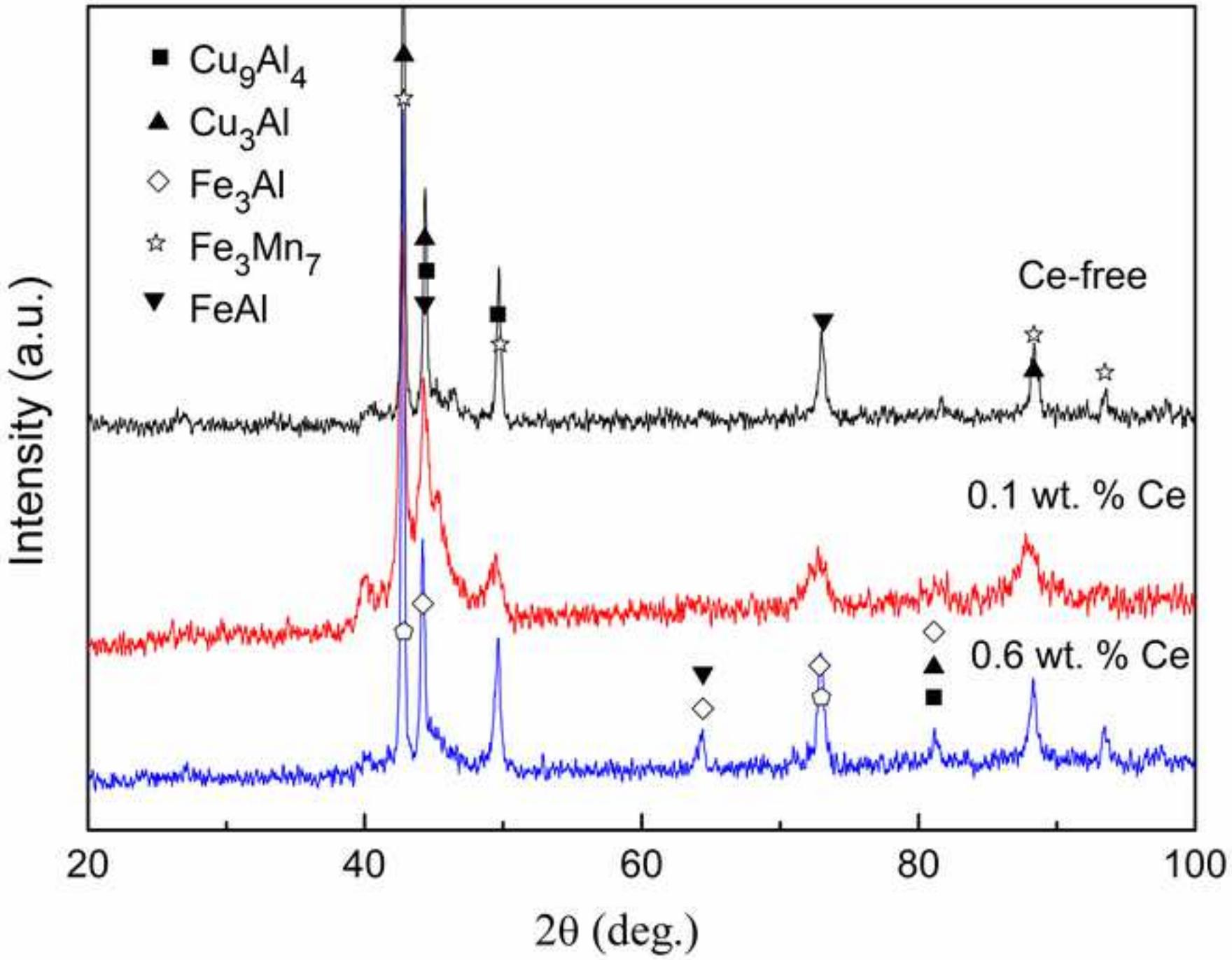

Figure 3

Click here to download Figure Fig. 3.tif

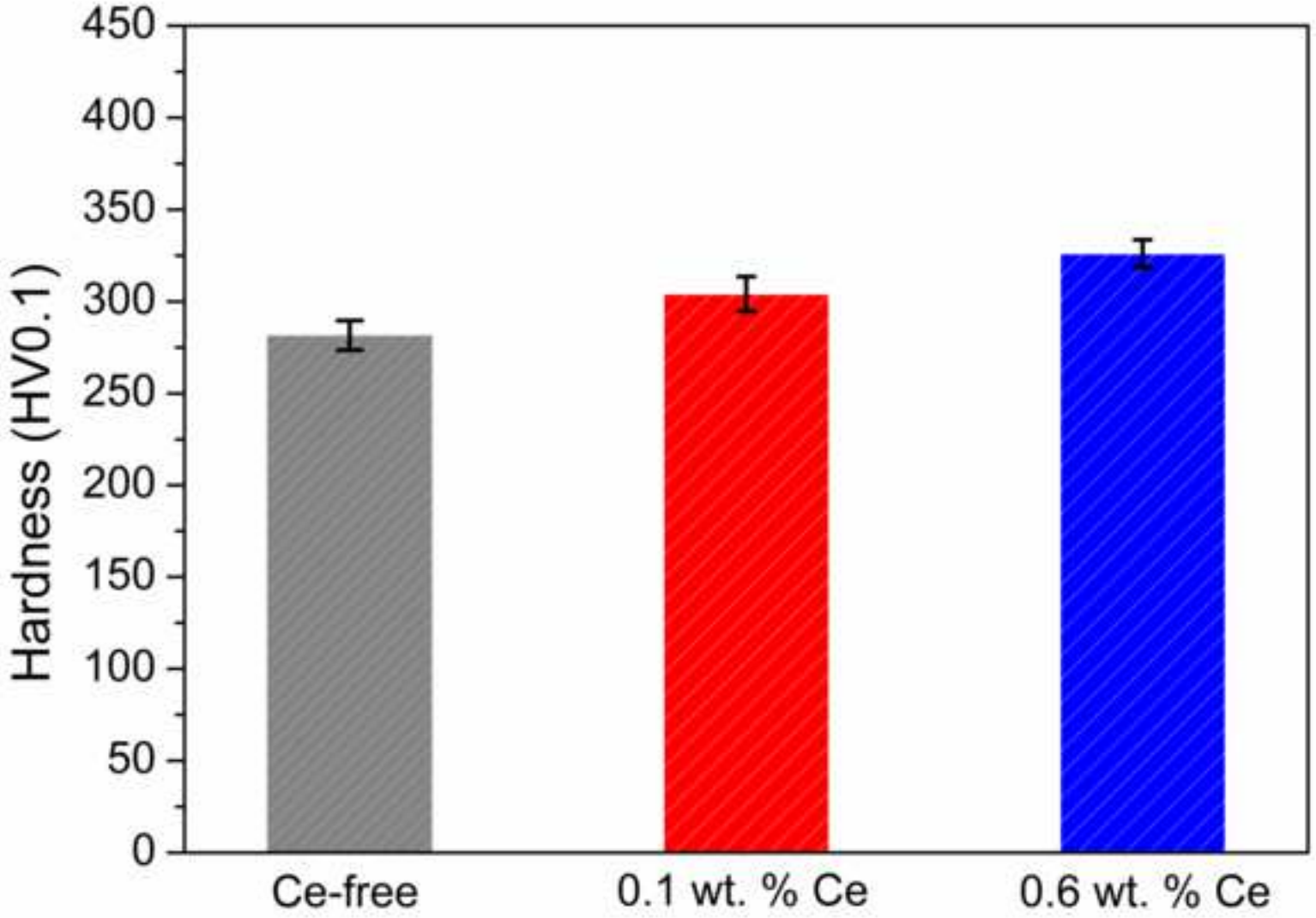

Figure 4

Click here to download Figure Fig. 4.tif

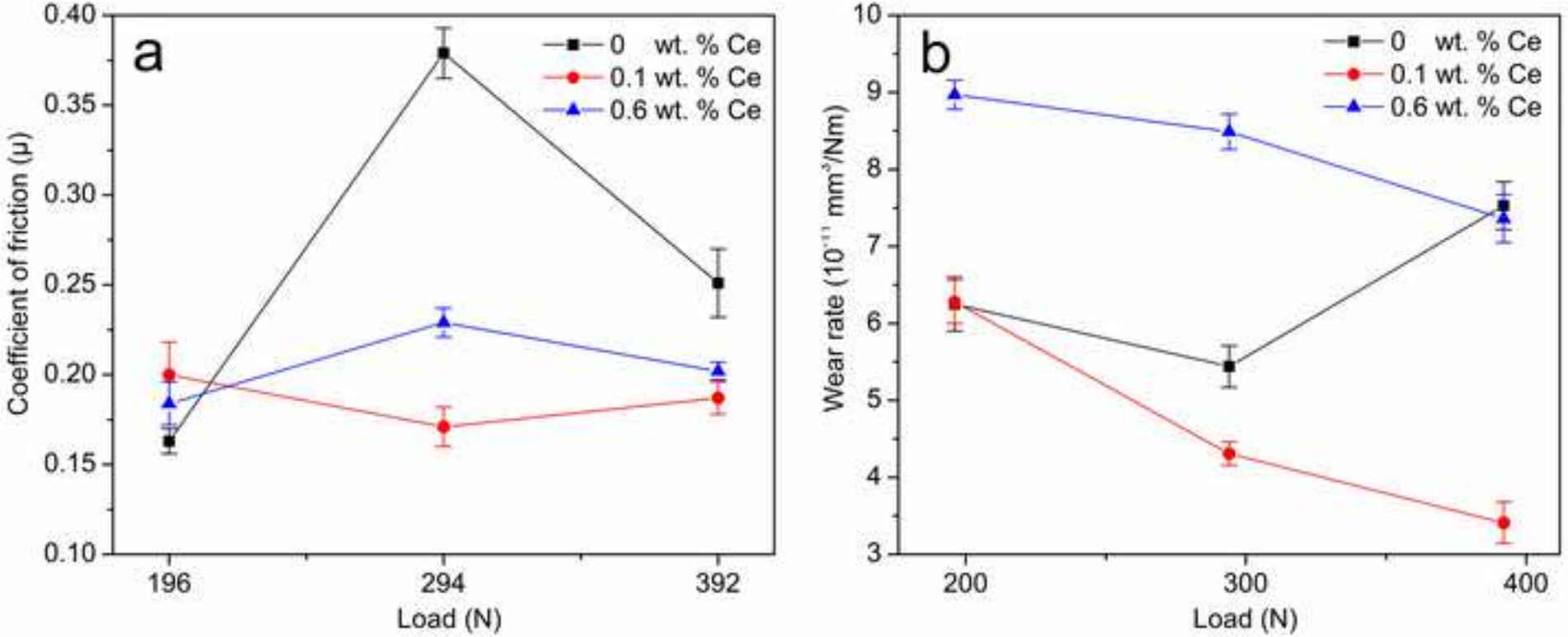

Figure 5

Click here to download Figure Fig. 5.tif

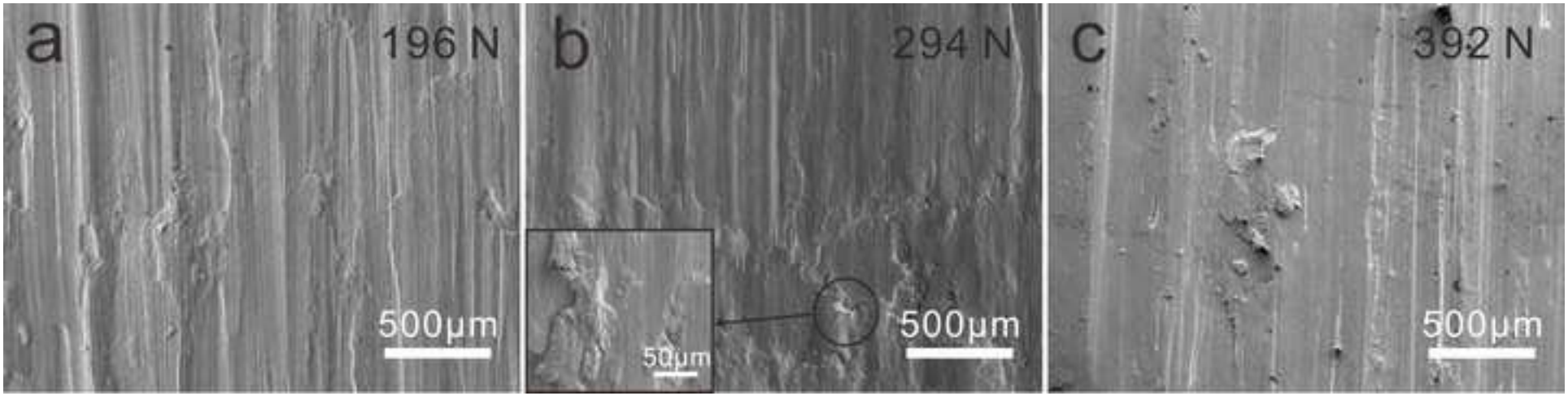

Figure 6

Click here to download Figure Fig. 6.tif

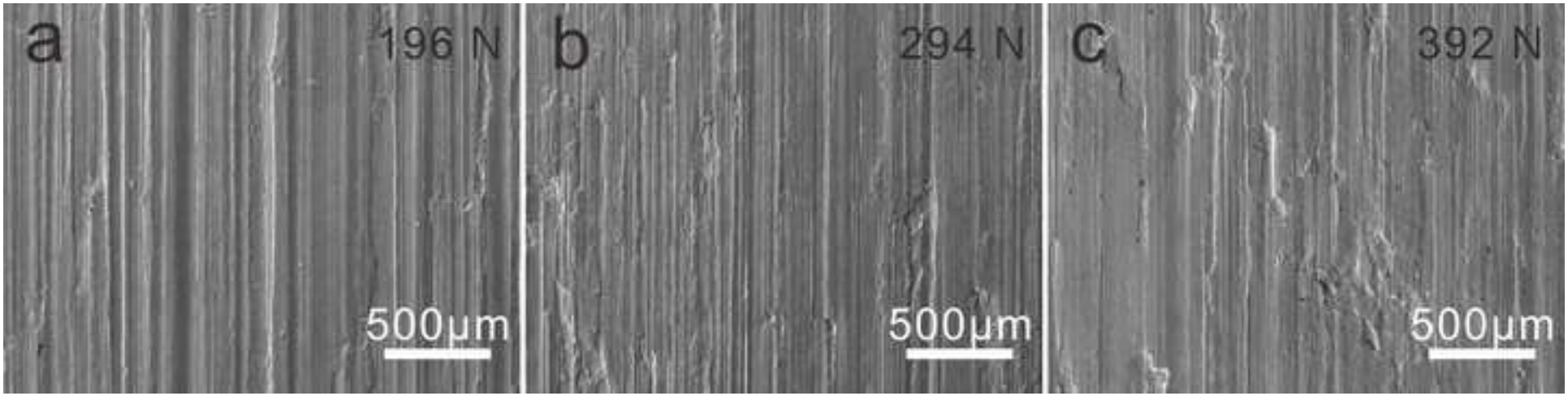

Figure 7

Click here to download Figure Fig. 7.tif

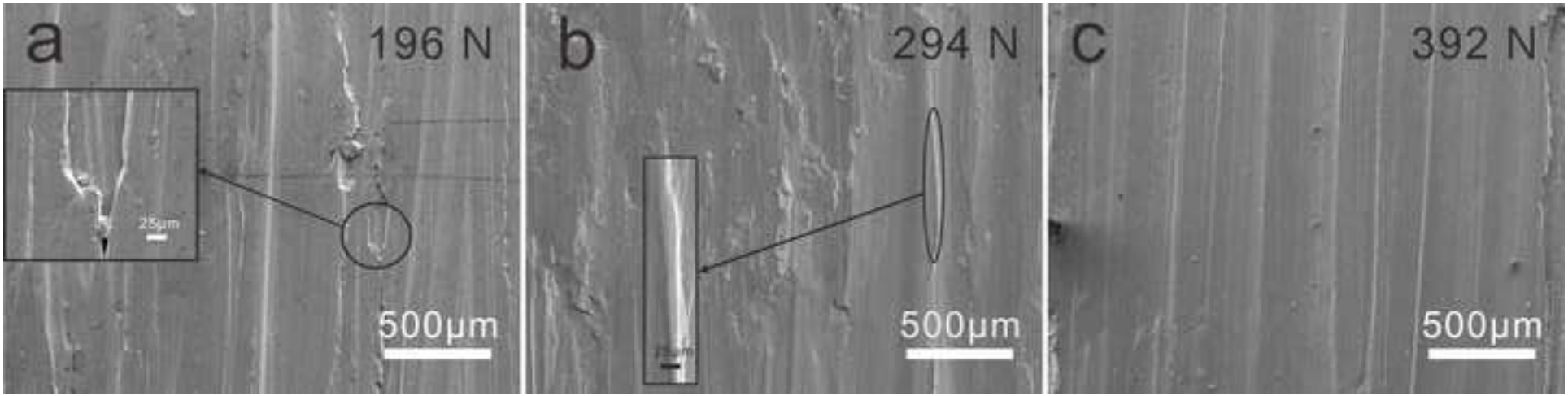

Figure 8

Click here to download Figure Fig. 8.tif

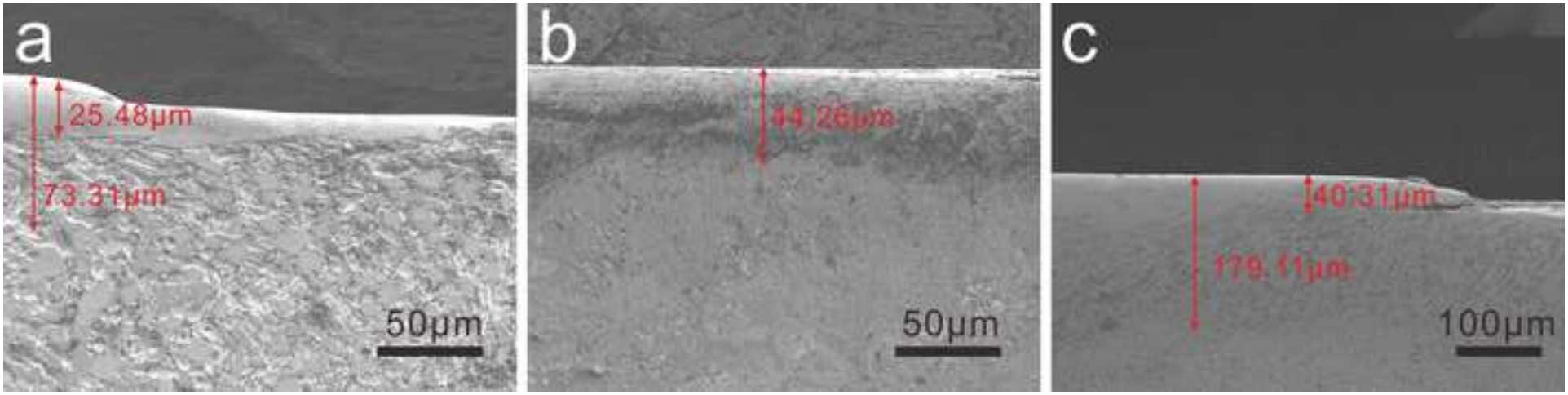

Figure 9

Click here to download Figure Fig. 9.tif

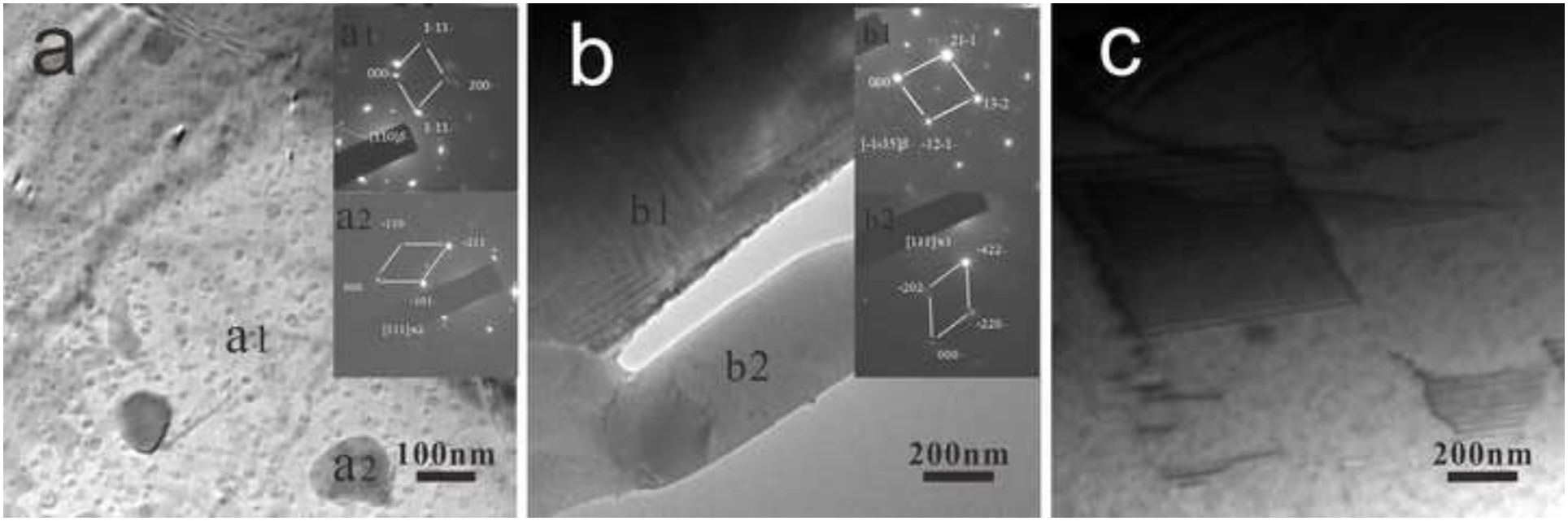

Figure 10

Click here to download Figure Fig. 10.tif

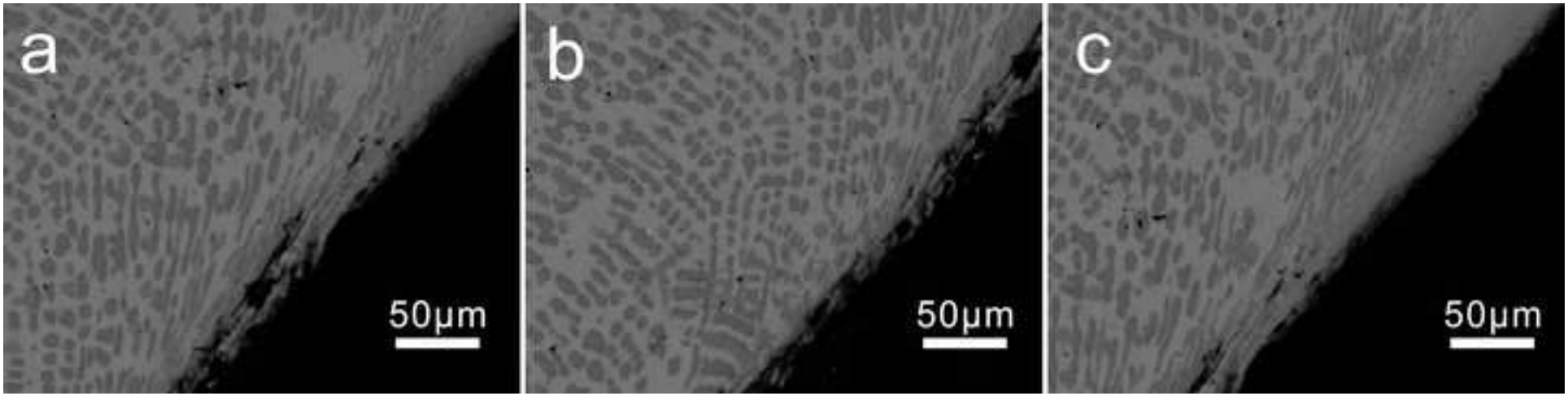

Figure 11

Click here to download Figure Fig. 11.tif

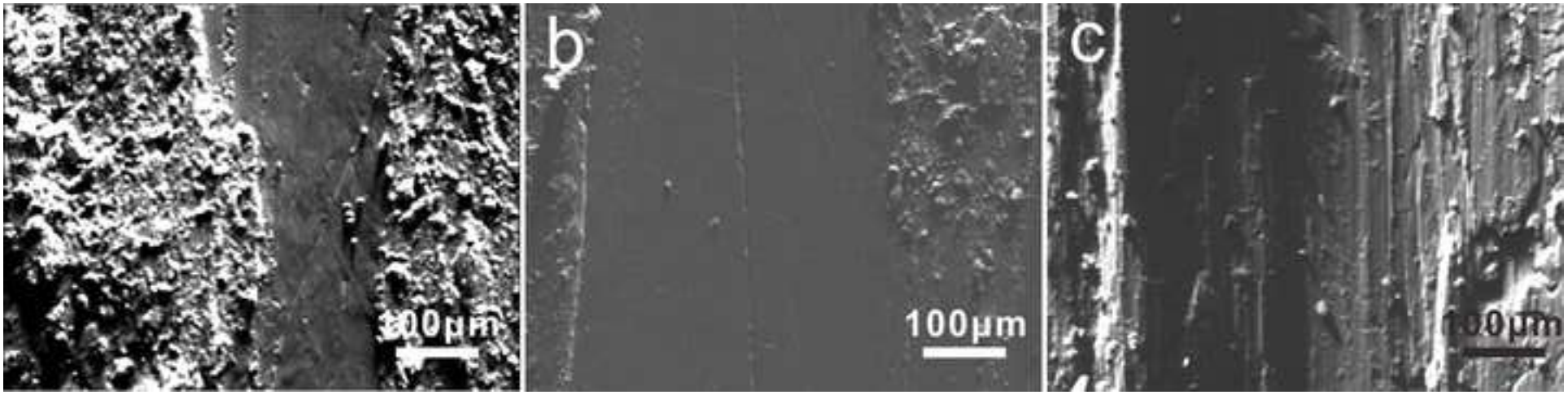

Figure 12

Click here to download Figure Fig. 12.tif

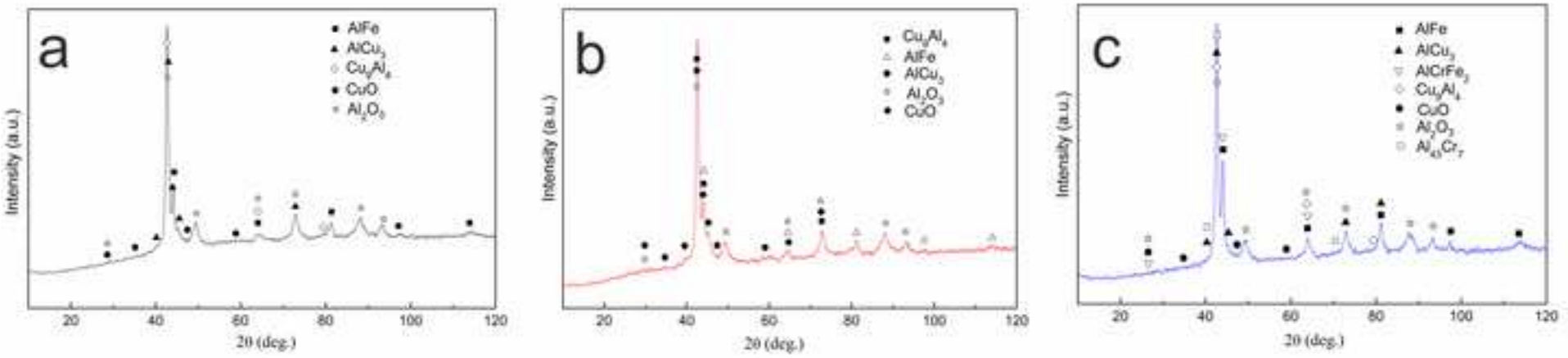

Figure 1

Click here to download Figure Figure 1.tif

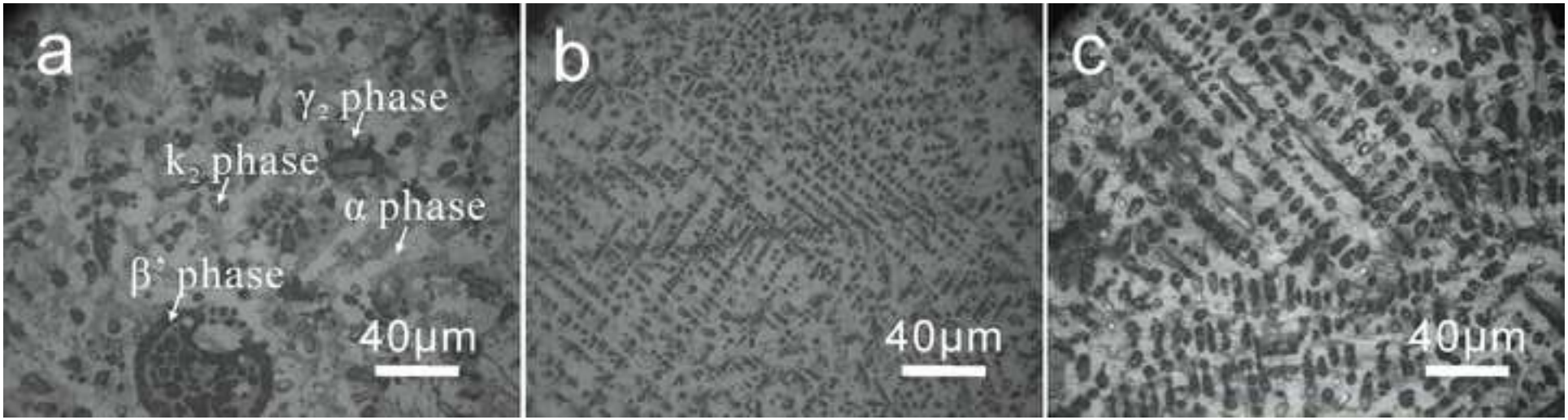

Table 1 Chemical composition of the Cu-14Al-4.5Fe-Ni alloy

Ingredients	Cu	Al	Fe	Co	Ni	Others
Weight percent (wt. %)	75~80	13~16	2.0~4.5	0.5-0.8	0.4~0.6	1.0~2.6

Table 2 Chemical composition of the substrate 1045 steel

Ingredients	Fe	Mn	C	Si	Ni	Cr	Cu	others
Weight percent (wt. %)	98.0~97.5	0.6~0.9	0.43~0.50	0.17~0.37	<0.25	<0.25	<0.25	<0.1

Table 2 Chemical compositions of the aluminum bronze coatings with different Ce contents (Ce-free, 0.1 wt. % and 0.6 wt. % Ce).

Coating	Chemical analysis, wt. %				
	Cu	Al	Fe	Ce	Others
0 wt. % Ce	67.5	9.9	20.0	0	2.6
0.1 wt. % Ce	66.7	10.1	20.5	0.1	2.5
0.6 wt. % Ce	60.6	10.1	26.7	0.6	1.9